PHYSICAL REVIEW C VOLUME 26, NUMBER 2 AUGUST 1982

Deuteron breakup by 140 MeV alpha particles at quasifree scattering conditions

J. M. Lambert and P. A. Treado
Department of Physics, Georgetown University, Washington, D.C. 20057

P. G. Roos, N. S. Chant, and A. Nadasen
Department of Physics and Astronomy, University of Maryland, College Park, Maryland 20742

I. Slaus
Department of Physics, Georgetown University, Washington, D. C. 20057
and Rudjer Boskovic Institute, 41001 Zagreb, Yugoslavia

Y. Koike
Department of Nuclear Engineering, Kyoto University, Kyoto, Japan
(Received 27 January 1982)

The ^{2}He$(\alpha,\alpha p)n$ reaction has been studied with 140 MeV alpha particles at p-α quasifree scattering conditions in the $\theta_{\text{c.m.}}$ angular region of 50° to 144°. Energy spectra are presented for six angle pairs. Three-body model calculations provide excellent fits to the data. Reasons for the success of the relatively limited three-body model used are discussed.

[NUCLEAR REACTIONS ^{2}H$(\alpha,\alpha p)n$, $E_\alpha=140$ MeV; measured $\sigma(E_\alpha,E_p,\theta_\alpha,\theta_p)$; three body Faddeev analysis; energy and angle dependence.]

I. INTRODUCTION

Three-body models based on the Faddeev equations[1] have been extended to systems of more than three nucleons, such as $\alpha+d$ (Refs. 2–5), ^{3}He + ^{6}Li (Refs. 6–8), and $p+^4$He (Ref. 9) with differing degrees of success. Among the significant reasons why these three-body model calculations do not always reproduce breakup and other data for such systems are the following: (1) In all these processes the Coulomb interaction plays a more important role than in the $p+d$ system and, at present, theoretical treatments do not adequately include Coulomb forces; (2) for energies above the particle breakup threshold energy, e.g., 20 MeV for α and 5 MeV for ^{3}He, a particle which is assumed to be structureless can actually disintegrate, thus opening additional reaction channels; and (3) particle-particle scattering data, which provide the needed input information for the three-body model calculations, lead to complex phase shifts as energies are increased or, as in the case of ^{3}He + ^{3}H in ^{6}Li, require complex phase shifts at all energies.

Despite these limitations the three-body model, as it has been applied to the $\alpha+d$ system, successfully predicts the ^{6}Li spectrum,[2] the position of the ^{6}He ground state,[3] $d+\alpha$ elastic scattering differential cross sections and polarization observables,[4] $d-\alpha$ (Ref. 5) breakup spectra at $E_\alpha=15$, 18, 27, and 42 MeV, and polarization observables in the $d+\alpha$ breakup.[10,11] Moreover, some of these data proved to be sensitive to the input nucleon-alpha (N-α) and nucleon-nucleon (N-N) forces; more specifically, the ground state binding energy and the vector analyzing power, $_iT_{11}$, in elastic $d+\alpha$ scattering depend on the deuteron D state probability, $P_d(D)$[4] [it is interesting to note that T_{22} seems to depend less on $P_d(D)$]. The inclusion of a $^1P_1$ term in the N-N force improves the fit of the three-body model predictions to the $d+\alpha$ elastic scattering data.[4]

Kinematically complete measurements of the deuteron breakup induced by alpha particles have been performed in the center of mass energy region from 5 to 55 MeV.[10–24] The energy correlation spectra are dominated by N-α quasielastic scattering (QFS) and N-α and N-N final state interactions (FSI). At higher c.m. energies the experimental data are described quite well by the modified impulse approximation prediction of Nakamura.[25] However, an inability to properly predict the low c.m. energy data necessitates the introduction of an additional reaction mechanism, triton transfer, and an additional F wave term in the n-p interaction. In contrast, the three-body model of Koike[5] adequately explains all the low c.m. energy data it has addressed.

Nadasen *et al.*[12] studied the $(\alpha,\alpha p)$ reaction on ^{2}H, ^{6}Li, and ^{19}F at $E_\alpha=140$ MeV. In this case, as

in our experiment, when the projectile is heavier than the constituent of the target undergoing QFS, the latter can be scattered at two different angles for a given scattering angle of the projectile. For these data, while the distorted wave impulse approximation (DWIA) provided satisfactory fits for those angle pairs where the proton is emitted at the larger QFS angle, it failed to predict a considerably broader spectrum measured for the ^{6}Li$(\alpha,\alpha p)$ reaction when the proton is emitted at the smaller QFS proton angle.

The aim of the present study is to investigate systematically the ^{2}H$(\alpha,\alpha p)n$ breakup reaction at c.m. energies considerably higher than the alpha particle binding energy. We will present α-p coincidence cross sections for both the small and large proton QFS angles at an incident energy of 140 MeV. These data are compared with (a) the plane wave impulse approximation (PWIA) (Ref. 26) using the experimental free α-p cross sections in the post collision prescription and (b) the three-body model of Koike.[5] The PWIA approach emphasizes the dominant feature of the physical QFS process and the omission of distortion effects is not too severe at this energy.[12] However, at lower energies the PWIA predicts a cross section which is too large not only for the ^{2}H$(\alpha,\alpha p)$ reaction, but also for all other QF processes measured below about 100 MeV c.m. energy. Three-body models, while oversimplifying the real many-nucleon system, do, indeed, include additional mechanisms which are not part of the PWIA (or the DWIA) approach. However, three-body models of the ^{2}H$(\alpha,\alpha p)n$ reaction do not take into consideration those reaction mechanisms which involve the alpha particle structure, e.g., triton transfer. To obtain a better insight into the three-body model we investigate the contribution of the α-p and α-n single scattering terms as well as the multiple scattering terms ending in n-p, n-α, and p-α final state interactions.

II. THEORY

A. Plane wave impulse approximation

The PWIA approach we use is described in detail in Ref. 26. It contains the square of the Fourier transform of the Hulthen deuteron wave function and the free proton-alpha elastic scattering cross section with post-collision energy. The elastic scattering data used in the PWIA analysis are summarized in Ref. 27.

B. Three-body model

The reaction ^{2}H$(\alpha,\alpha p)n$ can be considered as a three-body problem if the alpha particle is regarded as a structureless boson.[2–5] This model is described extensively in Refs. 5 and 28. It is based on the Alt-Grassberger-Sandhas formulation[29] and the resulting equations are solved by the rotated contour method.[30] The amplitude U describing the breakup process can be written as

$$U=I_{\alpha p}+I_{\alpha n}+M_{\alpha p}+M_{\alpha n}+M_{np} , \tag{1}$$

where I's are the first Born terms describing the α-p and α-n single scattering, and M's are the multiple scattering terms in which pairs indicated by subscripts interact in the final state of the reaction. We give explicit formulas for $I_{\alpha p}$ and $M_{\alpha p}$ in the Appendix. The impulse approximation (IA) is defined as taking into account only $I_{\alpha p}+I_{\alpha n}$. A strong destructive interference between $I_{\alpha p}$ and M_{np} observed at $E=18$ MeV (Ref. 13) suggests that it also is worthwhile to investigate the amplitude with no n-p FSI

$$G=I_{\alpha p}+I_{\alpha n}+M_{\alpha n}+M_{\alpha p} . \tag{2}$$

We first solve the three-body equation at $E_\alpha=140$ MeV. The input particle-particle forces are rank-one separable potentials with the Yamaguchi form factors for $s_{1/2}$, $p_{3/2}$, and $p_{1/2}$ states of the N-α subsystem and for the $^3S_1$ state in the N-N subsystem. Parameters of the nucleon-alpha interaction are listed in Table I of Ref. 5, i.e., potential CPV-A of Ref. 31 with modified values for $p_{1/2}$. Isospin conservation excludes the $^1S_0$ N-N force. It should be noted that the nucleon tensor force is not included in this model. The calculations include all amplitudes with $L\leq 7$, where L is the orbital angular momentum of the third particle relative to the interacting pairs.

The first term $I_{\alpha p}$ in Eq. (1) can be calculated independently of the solution of the three-body equation. The multiple scattering term $M_{\alpha p}$ contains a FSI factor $g_{\alpha p}\tau_{\alpha p}$ which is a multiplier. In the present paper some modifications to these terms are introduced (see the Appendix). Three types of p-α t matrices have been considered to calculate them.

(a) In the type I calculation, all two-body t matrices are obtained from the separable potential mentioned above. No correction is made for Coulomb effects. The QFS peaks at 140 MeV are

mainly influenced by p-α phase shifts above 20 MeV c.m. However, it is seen in Fig. 1 that the type I potential fails to reproduce experimental phase shifts in this energy region.[32–34]

(b) The type II calculation takes into account the fact that the proton and alpha are charged particles (see also Ref. 5) and determines p-α phase shifts from the following expression

$$C_l^2(\eta)k^{2l+1}\left[\cot\delta_l^{p\alpha}j+\frac{2\eta h(\eta)}{C_0^2(\eta)}\right]=a_{lj}+b_{lj}k^2+c_{lj}k^4+d_{lj}k^6\,, \tag{3}$$

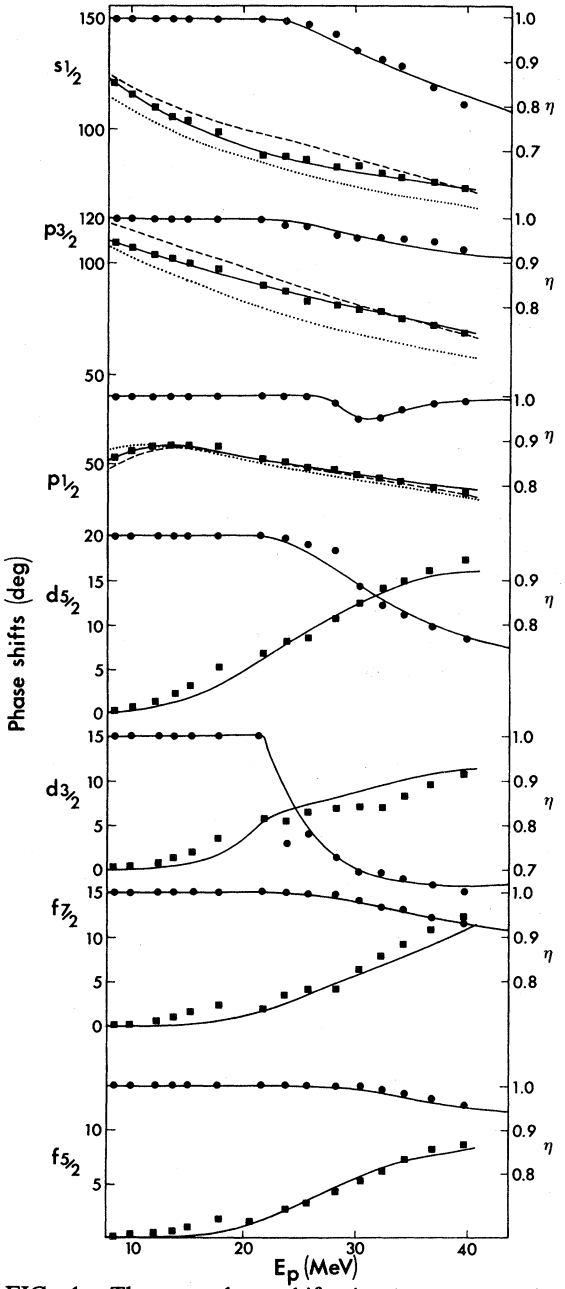

FIG. 1. The α-p phase shifts in degrees and the inelasticities η from Ref. 34. The curves are calculations using type I (dotted), type II (dashed), and type III (solid) α-p t matrices described in the text.

where a_{lj} to d_{lj} are given in Table I. Values for a_{lj} and b_{lj} are from Ref. 32. All other quantities have their usual meaning. Although these type II calculated phase shifts are in better agreement with the experimental phase shifts than the type I values, the p-α phase shifts have imaginary parts which are not included in the type II calculation. In the type II calculation the factor $\langle\bar{q}\,|\,Z\tau X\,|\,\bar{q}_{in}\rangle$ is again calculated using the modified CPV-A potential, but T_3 [see Eq. (A6)] and $g\tau$ [see Eq. (A11)] are calculated using the $s_{1/2}$, $p_{3/2}$, and $p_{1/2}$ phase shifts given by Eq. (3).

(c) The type III phase shifts are obtained as follows. Below 22 MeV, phase shifts are calculated as the type II phase shifts. Parameters are not the same as those of type II, but are from Ref. 33. Above 22 MeV we use simple formulas to fit the experimental phase shifts and inelasticities

$$\delta_{ij}=A_{lj}+B_{lj}E+C_{lj}E^2\,, \tag{4}$$

$$\eta_{lj}=1-\frac{X_{lj}E'^2}{(E'+Y_{lj})(E'+Z_{lj})}\,,\quad\text{except for } p_{1/2}\text{ wave}\,, \tag{5}$$

$$\eta_{11/2}=1-\frac{0.05624E'^2}{\{(E'-8.5)^2+5.866\}(E'+4.455)}\,, \tag{6}$$

with

$$E'=E-22\,,$$

where E is the proton energy in MeV and A_{lj}, B_{lj}, C_{lj}, X_{lj}, Y_{lj}, and Z_{lj} are parameters given in Table II. All effects neglected in the type II calculation are introduced in $I_{\alpha p}$. That is, the two-body t matrix in $I_{\alpha p}$ is calculated to fit the observed phase

TABLE I. Parameters used to obtain α-p phase shifts [see Eq. (3)] in type II calculations. Values of a_{lj} and b_{lj} are from Ref. 32; values of c_{lj} and d_{lj} are newly obtained.

	a_{lj}	b_{lj}	c_{lj}	d_{lj}
$p_{3/2}$	0.0223065	−0.1825	0.30	0.28
$p_{1/2}$	0.9516529	0.1745	0.29	0.63
$s_{1/2}$	−0.201207	0.6475	−0.41	0.307

shifts including imaginary parts up to $l=3$. As for M_{ap} we again use s and p wave t matrices, but we modify $q\tau$ using the observed p-α phase shifts including the imaginary parts. It should be noted that the inelasticity parameter, η, is appreciably different from unity for incident proton energies larger than 25 MeV. Also the n-α interaction is described by the CPV-A potential, i.e., the types II and III calculations treat it in the same manner as the type I calculation. The n-p t matrix is also kept the same for the types I, II, and III calculations.

III. EXPERIMENTAL APPARATUS AND PROCEDURES

A. Accelerator, scattering chamber, and target

The analyzed 140 MeV alpha particle beam from the University of Maryland (UMD) cyclotron was used to bombard a 12 cm diameter gas cell with 0.008 mm Havar windows containing deuterium gas at 1 atm. One of the UMD 152 cm scattering chambers was used with a halo aperature at the entrance to the chamber. A Faraday cup collected the beam approximately 4 m downstream. Beam alignment was monitored periodically with TV viewing of a BeO scintillator target and with two-body elastic scattering coincidence data.

The ^{2}H gas cell was flushed twice before being filled for data accumulation and its pressure was monitored continuously during each experimental run. Its pressure variation was less than 1.5% during each run. There was a small amount of hydrogen gas contamination, less than 0.5%, which was observed when the appropriate two-body $\alpha+p$ coincidence angles were used.

B. Detection system

Two detector telescopes were used in this experiment. For alpha particles the detecting telescope consisted of a 150 μm Si surface barrier ΔE detector and a 2000 μm Si surface-barrier E detector. For detecting protons, a 1000 μm Si surface-barrier ΔE detector and a 1.9 cm diameter by 5 cm thick NaI E detector were used. The resolution of the NaI detector had been previously measured to be 650 keV for 65 MeV protons.[35–37]

The p and α telescopes were positioned at 28 and 40 cm, respectively, from the center of the scattering chamber. In order to exclude events originating in the gas cell windows two collimators were used for each telescope. For the proton arm, the front collimator (0.27 cm wide by 0.80 cm high) was 13 cm from the center of the gas cell while the second collimator (0.40 cm wide by 0.80 cm high) was 15 cm behind the first. For the alpha particle arm, the front collimator was 10.8 cm from the center of the gas cell and the second collimator was 29.2 cm behind the first, each having a circular 0.63 cm diameter opening.

The detector telescopes, biased for total depletion of each surface barrier detector and for optimal resolution of the NaI detector, were utilized with standard coincidence electronics and with five analog signals, ΔE_p, E_p, ΔE_α, E_α, and time-to-amplitude converter (TAC), routed to the computer. The resolving time of the system was sufficient to distinguish between adjacent rf cycles of the cyclotron, so accidental coincidences could be subtracted from the total coincidence spectrum by software gating. Also, pulsers for each detector, triggered by one tenth of the current integration pulses, were routed through the system for inclusion in each spectrum to allow dead time corrections for the data.

Calibration of both energy axes was obtained by observing two-body elastic $\alpha+d$ scattering and by the presence of a small hydrogen contamination in the deuteron gas cell which provided sharp two-body coincidence structure in some of the three-body breakup spectra.

It should be noted that high energy charged parti-

TABLE II. Parameters used to fit the experimental α-p phase shifts in type III calculations for proton energies greater than 22 MeV [see Eqs. (4), (5), and (6) of text].

	A	B	C	X	Y	Z
$s_{1/2}$	115.41	−1.409	0.009475	0.5550	9.509	18.86
$p_{3/2}$	115.05	−1.306	0.005376	0.2873	5.958	33.87
$p_{1/2}$	66.06	−0.6804	0.000506			
$d_{5/2}$	−10.68	0.8817	−0.004535	0.5900	7.023	15.24
$d_{3/2}$	−1.41	0.3646	−0.000990	0.3982	1.046	1.706
$f_{7/2}$	−10.72	0.6184	−0.002232	0.5242	21.37	40.18
$f_{5/2}$	−20.48	1.328	−0.01539	1.175	63.21	78.68

cles, when detected in NaI(Tl) or silicon counter, can leave a signal which is smaller than that which would be proportional to their energy because the particle can have nuclear interactions with the detection medium nuclei. The calculations of the corrections due to these losses have been performed[38] for protons, deuterons, and alpha particles for both silicon and NaI detectors. Some measurements[39] also exist which demonstrate, in general, a good agreement with the calculations. In our experiment corrections for these losses as well as for out-scattering effects ranged from 3 to 11%, introducing a systematic error of less than 3%.

IV. DISCUSSION AND RESULTS

We have investigated α-p QFS in the angular region from $\theta_{\text{c.m.}}=50°$ to 144°. Six energy correlation spectra are shown in Figs. 2–7 together with the predictions of type III calculations. The error bars shown are statistical errors. The systematic errors, including uncertainties due to the product of solid angles and effective target thickness, to the current integration, to the reaction and out-scattering correction, to dead time corrections, and to possible variation in the beam width at the target during the measurement, amount to $<12\%$.

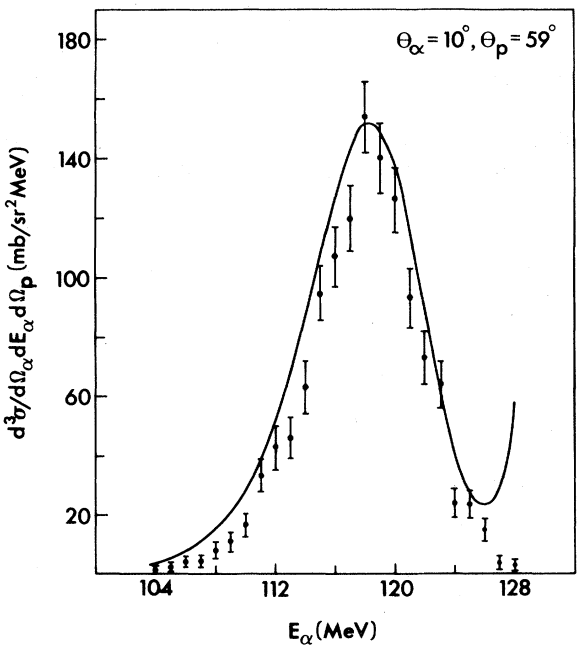

FIG. 2. Energy correlation spectrum for the reaction ^{2}H(α,αp)n with $\theta_\alpha=10°$ and $\theta_p=59°$ projected on the alpha axis. Only statistical errors are shown. The solid curve represents the predictions of the type III calculation.

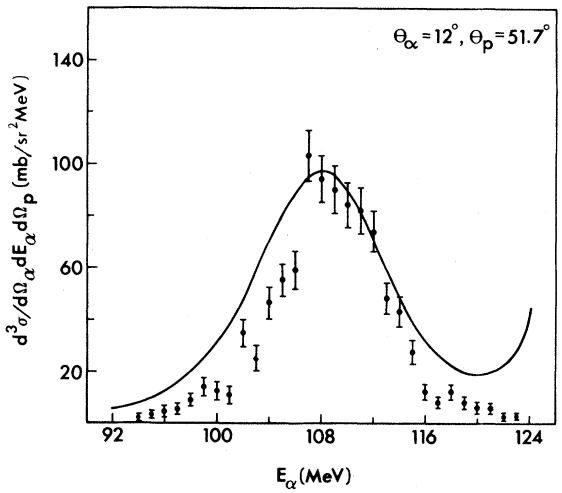

FIG. 3. Same as Fig. 2 except $\theta_\alpha=12°$, $\theta_p=51.7°$.

Each spectrum shows a pronounced peak at the α-p QFS conditions, demonstrating that this is a dominant process at the incident energy of 140 MeV, when appropriate kinematics conditions are selected.

From the experimentally measured differential cross section $d\sigma^3/d\Omega_\alpha dE_\alpha d\Omega_p$ and using the general structure of the PWIA cross section, one can extract the square of the Fourier transform for the deuteron wave function. Data, summarized in Fig. 8, show that the quasifree scattering is indeed a dominant mechanism at least in the domain where the momentum transfer is less than 0.3 fm^{-1}. The

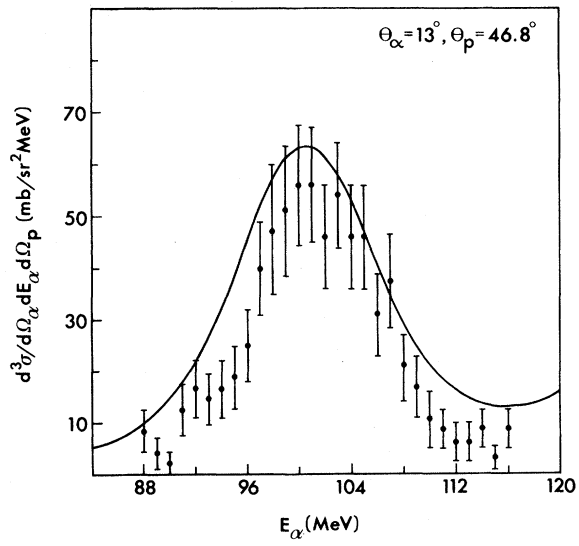

FIG. 4. Same as Fig. 2 except $\theta_\alpha=13°$, $\theta_p=46.8°$.

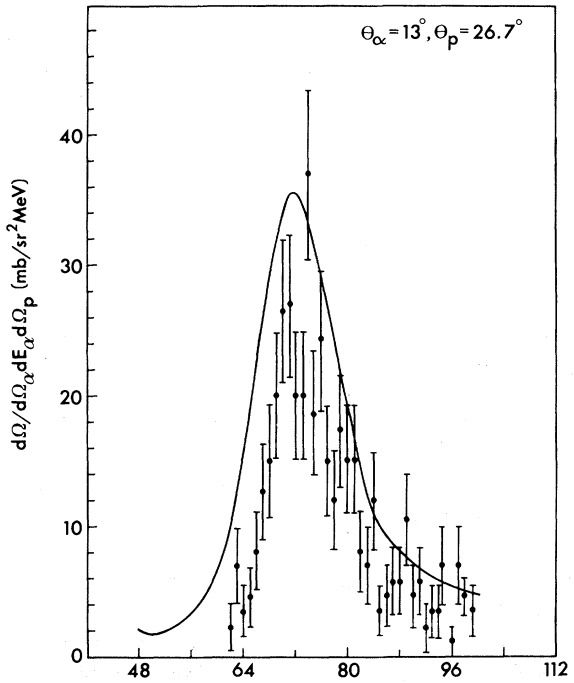

FIG. 5. Same as Fig. 2 except $\theta_\alpha = 13°$, $\theta_p = 26.7°$.

comparison between these data and the calculated square of the Fourier transform of the Hulthen deuteron wave function shows that the PWIA overestimates the absolute cross section by a factor

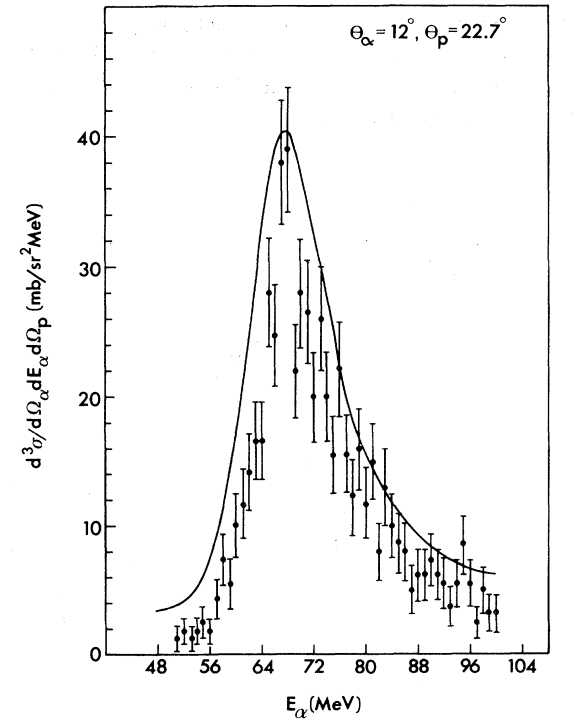

FIG. 6. Same as Fig. 2 except $\theta_\alpha = 12°$, $\theta_p = 22.7°$.

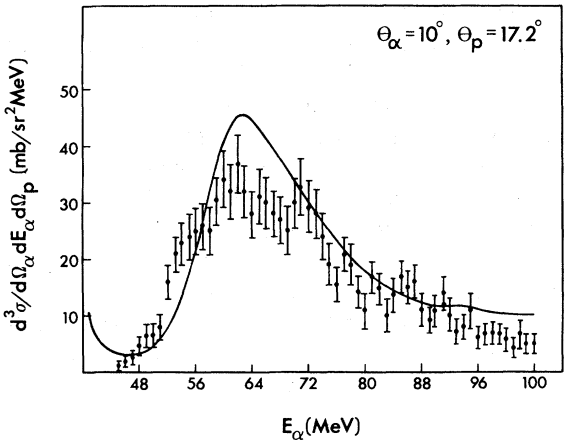

FIG. 7. Same as Fig. 2 except $\theta_\alpha = 10°$, $\theta_p = 17.2°$.

$N^{-1} = 1.79$, and that, in general, the data indicated a narrower distribution. Both features have been established for many quasifree processes involving light nuclei in this energy region (see, cf., Ref. 26).

Figures 2–7 demonstrate a rather striking fit which a type III three-body calculation achieves. The lack of any serious discrepancy requires some further discussion in view of the assumptions in our model; that is, the structure of the alpha particle is ignored and no tensor *n-p* force is included. In Figs. 9 and 10 we show the individual contribution of the terms $I_{\alpha p}$, $I_{\alpha n}$, $M_{\alpha p}$, $M_{\alpha n}$, and M_{np} to the cross section at two angle pairs. Note that the terms are amplitudes and do not contain a phase space factor. An important feature of these (and all other) correlation spectra is the dominance of the $I_{\alpha p}$ term (note that even a different scale is used).

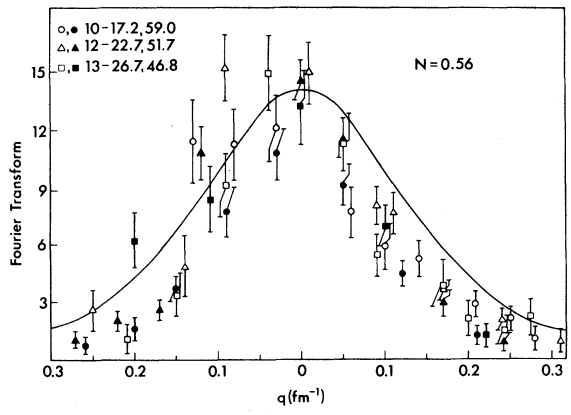

FIG. 8. Extracted square of the Fourier transform from the cross section measurements of the ^{2}H(α,αp)n reaction at α-p QFS conditions. The data from the various angle pairs are represented with different symbols. The solid curve is a prediction using a Hulthen deuteron S-wave function with the normalization factor $N = 0.56$.

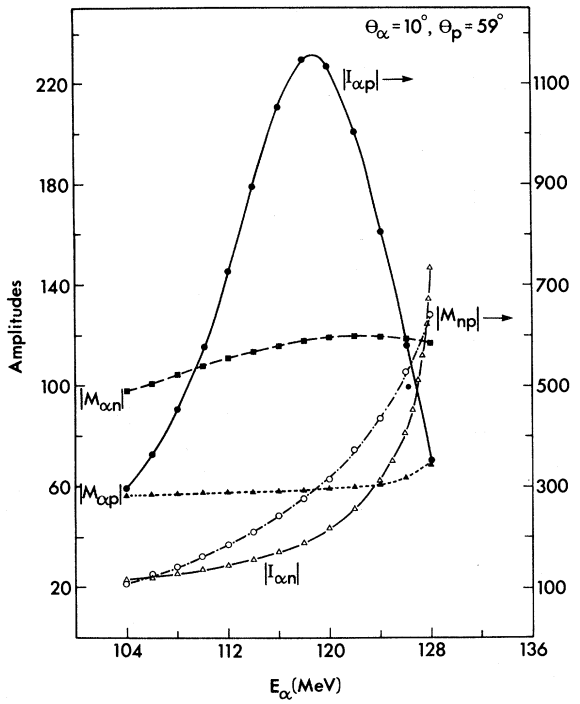

FIG. 9 Contribution of the individual terms, I_{ap}, I_{an}, M_{ap}, M_{an}, and M_{np} to the differential cross section for $\theta_\alpha = 10°$, $\theta_p = 59°$. The amplitudes are complex numbers depending on kinematical variables, but only the absolute values of each term are plotted here. The cross section is obtained by taking the square of the absolute value of all these terms and multiplying with the kinematical factor.

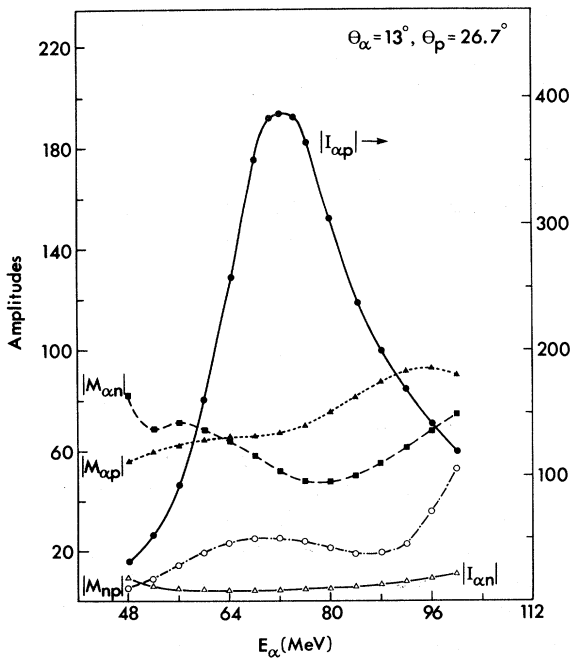

FIG. 10. Same as Fig. 9 except $\theta_\alpha = 13°$, $\theta_p = 26.7°$.

All multiple scattering terms slowly vary with the detected particle energy and they generally interfere destructively with I_{ap}. The term I_{ap} is essentially equal to the PWIA, when squared and multiplied by a phase space factor. Any differences arise from small differences between the experimental p-α cross section used in the PWIA and the off-energy-shell p-α t matrix used in I_{ap}.

Since I_{ap} is the main component, the quality of the fit depends crucially on it. Comparisons between types I, II, and III calculations in Figs. 11 and 12 demonstrate that the correct *absolute* cross section can be obtained only by using p-α phase shifts which fit the two-body data. This underlines also the importance of careful measurements of the experimental absolute $(\alpha,\alpha p)$ cross section, since even types I and II calculations would be able to explain the *shape* of the spectra. For all QFS conditions that we have studied except $\theta_\alpha = 13°$, $\theta_p = 26.7°$, and $\theta_{\text{c.m.}} = 124.3°$, the cross section predicted by the type III calculations are smaller than those predicted by types I and II. Cross sections predicted by types I and II calculations are

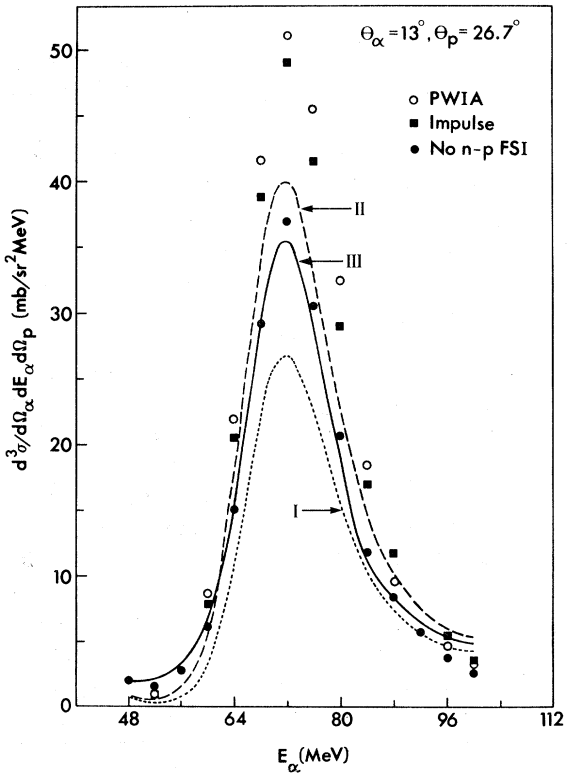

FIG. 11. Comparison of prediction of types I (dotted), II (dashed), and III (solid) calculations; of type III without n-p FSI (solid circles); of impulse approximation ($I_{ap}+I_{an}$: closed squares) and PWIA with Hulthen wave function (open circles) for $\theta_\alpha = 13°$, $\theta_p = 26.7$.

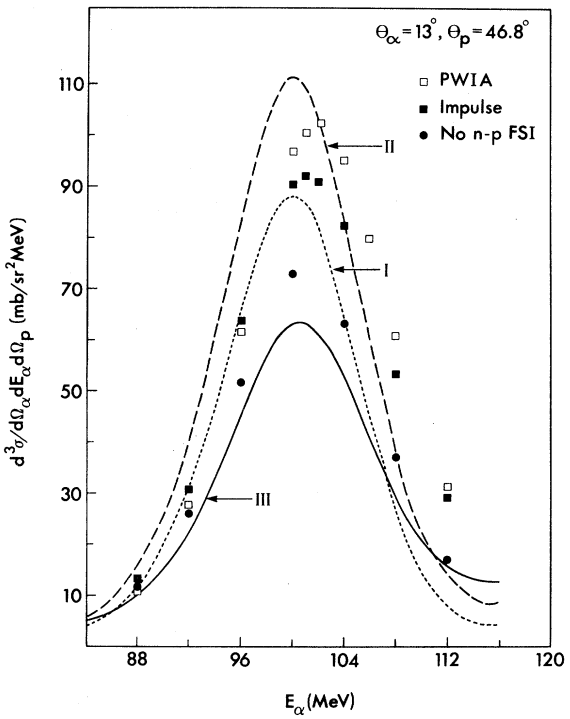

FIG. 12. Same as Fig. 11 except $\theta_\alpha = 13°$, $\theta_p = 46.8°$.

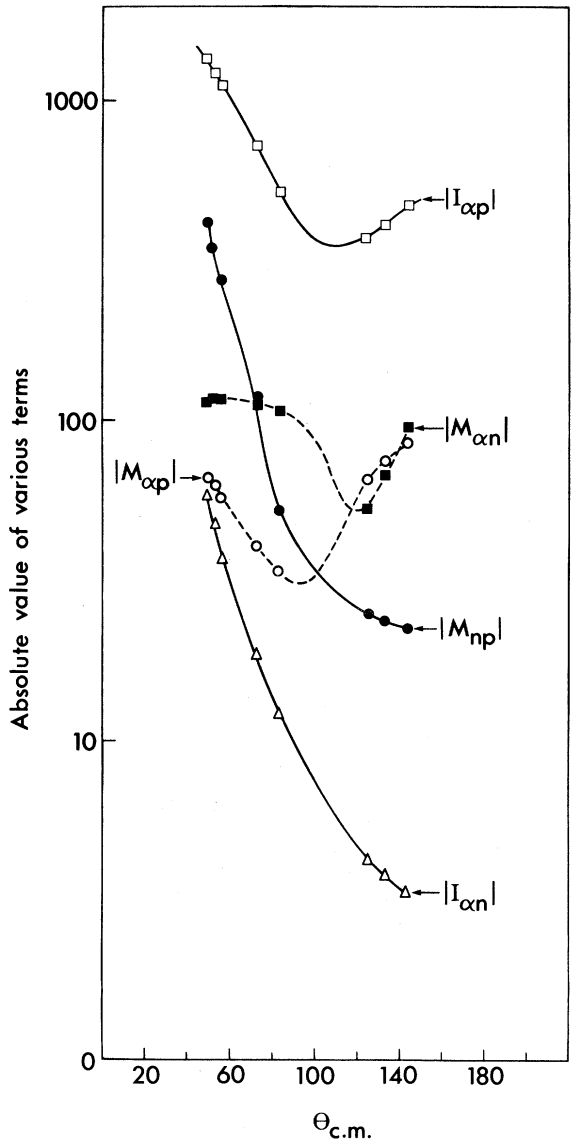

FIG. 13. Angular variation of the absolute values of the individual terms contributing to the cross section as a function of the α-p c.m. angle, $\theta_{c.m.}$.

typically 12—60% and 30—100% larger, respectively, than those predicted by the type III calculation.

The angular variation of absolute values of individual terms contributing to the cross section is shown in Fig. 13. The term M_{np} is quite important at small $\theta_{c.m.}$ angles. The pronounced angular dependence of M_{np} shows that many partial waves contribute to M_{np}.

At small $\theta_{c.m.}$ the n-p FSI is very important and M_{np} amounts to 30% of $I_{\alpha p}$. A strong destructive interference between $I_{\alpha p}$ and the amplitude which describes the n-p FSI was first pointed out in Ref. 16 on the basis of the modified impulse approximation. A full discussion of this interference is given in Ref. 40, where its strength is related to the weakness of the deuteron binding. That is, because the deuteron is a loosely bound system, the incident alpha particle interacts only with a proton, leaving a neutron as a spectator. However, since the range of the deuteron wave function is large because of its low binding energy, the recoil proton can still interact with the neutron. Thus, the neutron does not remain a spectator, and a strong n-p FSI reduces the QFS peak. This effect depends on $\theta_{c.m.}$ and it is particularly strong at small angles.

Figure 14 shows the angular dependence of the QFS peak cross section together with the three-body model prediction with all terms included ($I + M_{\alpha p} + M_{\alpha n} + M_{np}$), with the n-p FSI omitted ($I + M_{\alpha n} + M_{\alpha p}$), and with a combination of the impulse approximation term plus either $M_{\alpha p}$ (i.e., $I + M_{\alpha p}$) or $M_{\alpha n}$ (i.e., $I + M_{\alpha n}$). Note, that while at small $\theta_{c.m.}$ I (more precisely $I_{\alpha p}$) and M_{np} are dominant, at $\theta_{c.m.} \sim 80° - 150°$ all terms are important. The full three-body model predicts the experimental angular distribution quite well except at $\theta_{c.m.} = 144°$ ($\theta_\alpha = 10°$, $\theta_p = 17.2°$).

It is at large $\theta_{c.m.}$ that one expects the structure of the alpha particle to become important. Howev-

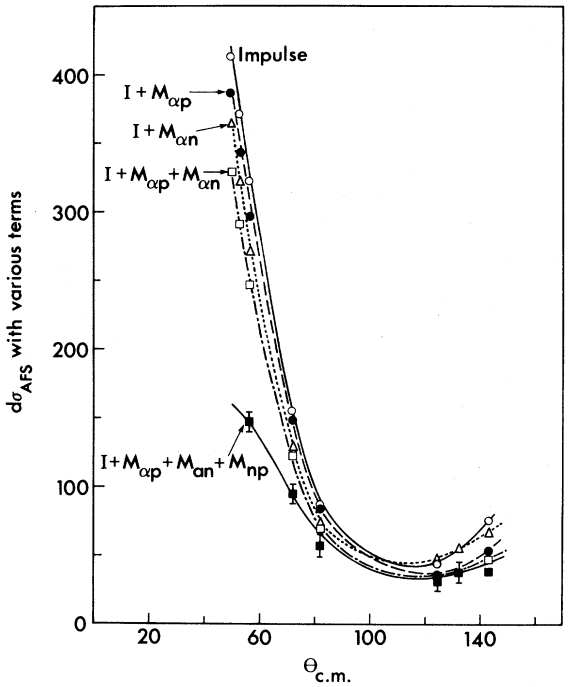

FIG. 14. Angular dependence of the QFS peak cross section together with the predictions of the three body model where all terms are included ($I+M_{np}+M_{\alpha p}+M_{\alpha n}$), where n-p FSI is omitted ($I+M_{\alpha p}+M_{\alpha n}$), and where either the $M_{\alpha p}$ or the $M_{\alpha n}$ term is included with the impulse approximation terms. The data are represented by the solid squares with the error bars. The $\theta_{c.m.}$ is as in Fig. 13.

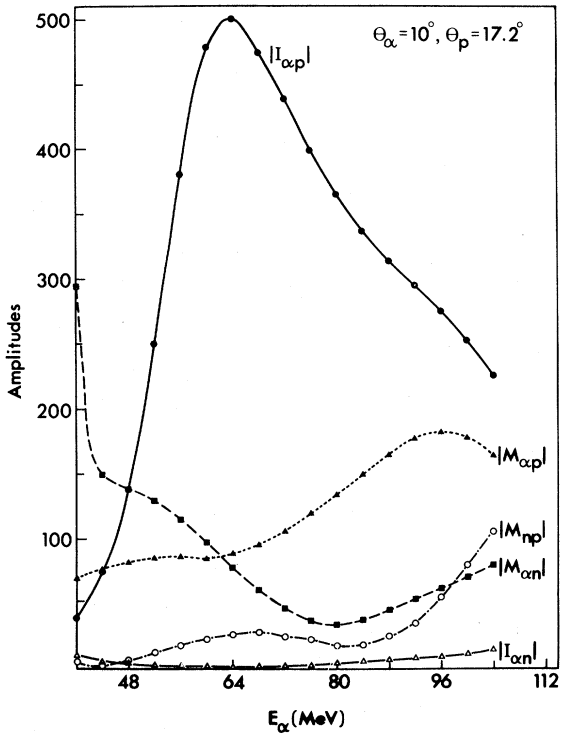

FIG. 15. Same as Fig. 9 except $\theta_\alpha=10°$, $\theta_p=17.2°$.

V. CONCLUSIONS

The fits of the three body model[5] to the 140 MeV QFS data are quite good, while the same model did

er, it is possible that further improvements in the three-body model, e.g., better treatment of the n-α interaction and the n-p tensor force, can improve the fit of the $\theta_\alpha=10°$, $\theta_p=17.2°$ data. The large contribution of $M_{\alpha n}$ at $E_\alpha\sim40-65$ MeV to the cross section shown in Fig. 15 suggests that improvements in the treatment of the n-α interaction can indeed improve the three-body model. For instance, a better n-α two-body t matrix may be useful.

The comparison of the three-body model to the data in Figs. 2–7 suggests that except for $\theta_\alpha=10°$, $\theta_p=17.2°$, the experimental QFS peaks are somewhat narrower than predicted. Similar features have been found in many quasifree processes. Figure 16 shows the ratio of the full-width-half-maximum of the QFS data and the three-body model as a function of $\theta_{c.m.}$. The fact that the ratio is less than one over a wide range of $\theta_{c.m.}$ suggests that other improvements in our theoretical model, besides inclusion of the structure of the alpha particle, are necessary.

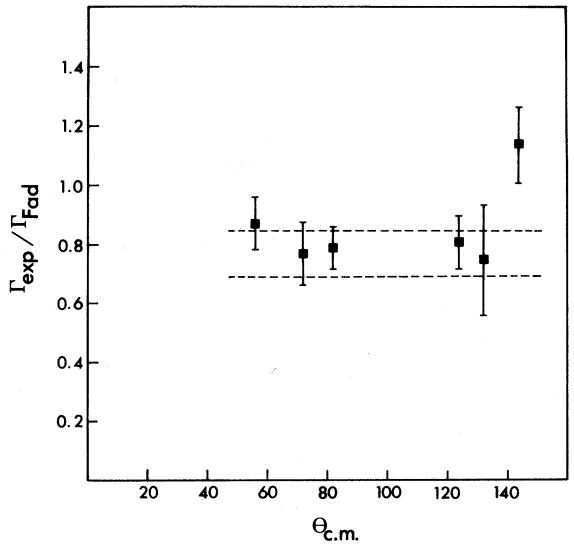

FIG. 16. Ratio of the full-width-half maximum, Γ, of the α-p QFS data and the three-body-model as a function of the $\theta_{c.m.}$ given in Fig. 13. The area between the dashed lines represents the region where PWIA predictions lie.

not fit the QFS data well for $E_\alpha=29$ MeV (Ref. 19) and $E_\alpha=42$ MeV (Ref. 20). Recently, preliminary QFS data at $E_\alpha=28$ MeV (Ref. 41) have been reproduced better by the model. At 140 MeV the impulse approximation is better than at lower energies and contributions of other terms are, consequently, less important than at lower energies. However, a determination of the sensitivity of the results to an improved n-α two-body t matrix is suggested. Also, at higher energies the effect of the alpha particle structure becomes important. It would be desirable to have additional data between 50 MeV and 150 MeV and to be able to investigate other angular correlation data at 140 MeV.

ACKNOWLEDGMENTS

The computer calculations of the theoretical three-body model predictions for this work were financially supported by the Research Center for Nuclear Physics, Osaka University. The research was partially supported by National Science Foundation (NSF) grants at the University of Maryland and (Phy 77-03903) at Georgetown University. Some NSF (grant F6F005 PL 480) monies were used for travel. Appreciation for the support and cooperation rendered by the operational staff of the UMD cyclotron and computer facilities is noted. Finally, the authors acknowledge the help of Dr. T. A. Carey, Dr. L. T. Myers, and Mr. M. Elhawamdah.

APPENDIX

In this appendix we give an explicit formula for $I_{\alpha p}$ and $M_{\alpha p}$. Let us define the particle channels as follows:

$$\alpha+(p,n)$$

corresponding to channel 1,

$$p+(n,\alpha) \tag{A1}$$

corresponding to channel 2, and

$$n+(p,\alpha)$$

corresponding to channel 3.

The breakup amplitude in (AGS) formalism is

$$U_{01}=(E-H_0)+\sum_c T_c G_0 U_{c1}\ , \quad (c=1,2,3)\ , \tag{A2}$$

where

$$U_{c1}=(1-\delta_{c1})(E-H_0)+\sum_{c'\neq c} T_{c'} G_0 U_{c'1}\ . \tag{A3}$$

The amplitude U_{01} must be bracketed by the final state $\langle \vec{q}\vec{p}\,|$ and initial state $|\,\phi\rangle$

$$U=\langle \vec{q}\vec{p}\,|\,U_{01}\,|\,\phi\rangle=\sum_c \langle \vec{q}\vec{p}\,|\,T_c G_0 U_{c1}\,|\,\phi\rangle\ . \tag{A4}$$

Here we have used the fact that the first term of Eq. (A2) vanishes on the energy shell.

Substituting (A3) into (A4), we obtain

$$U=\sum_{c=2,3}\langle \vec{q}\vec{p}\,|\,T_c\,|\,\phi\rangle + \sum_{c,c'}\vec{q}\vec{p}\,|\,T_c G_0 T_{c'} G_0 U_{c'1}\,|\,\phi\rangle\ . \tag{A5}$$

Then the first Born term $I_{\alpha p}$ is

$$I_{\alpha p}=\langle \vec{q}\vec{p}\,|\,T_3\,|\,\phi\rangle=\int\int d\vec{q}\,'d\vec{p}\,'\langle \vec{q}\vec{p}\,|\,T_3\,|\,\vec{q}\,'\vec{p}\,'\rangle\langle \vec{q}\,'\vec{p}\,'\,|\,\phi\rangle\ , \tag{A6}$$

where the first factor is the half off shell two-body t matrix in the three-body Hilbert space

$$\langle \vec{q}\vec{p}\,|\,T_3\,|\,\vec{q}\,'\vec{p}\,'\rangle=\delta(\vec{q}-\vec{q}\,')T_{\alpha p}(p,p';P^2/2\mu_{\alpha p})\ , \tag{A7}$$

and the second factor is the same deuteron wave function as used in PWIA. The off shell two-body t matrix can be calculated from the separable potential. When we modify the t matrix we assume the partial wave off shell t matrix is related to the on shell one by

$$t_{lj}(p,p;k^2/2\mu)=g_{lj}(p)g_{lj}(p)g_{lj}^{-2}(k)t_{lj}(k,k,k^2/2\mu)\ , \tag{A8}$$

with

$$g_{lj}(p)=p^l/(p^2+\beta_{lj}^2)^2 \quad (l=0,1)\ ,$$

and

$$g_{lj}(p)1 \quad (l\geq 2)\ . \tag{A9}$$

The parameters β are the same as those of the input separable potential in the three-body equation.

The multiple scattering amplitude $M_{\alpha p}$ can be written

$$M_{\alpha p}=\sum_{c=1,2}\langle \vec{q}\vec{p}\,|\,T_3G_0T_cG_0U_{c1}\,|\,\phi\rangle\ . \qquad \text{(A10)}$$

For the separable potentials Eq. (A10) becomes

$$\langle n\,|\,M_{\alpha p}\,|\,r\rangle=g_{3n}(\vec{p})\tau_{3n}(P^2/2\mu_{\alpha p})\times\sum_{c,m}\langle \vec{q}\ Z_{3ncm}\tau_{3n}X_{cmlr}\,|\,\vec{q}_{in}\rangle\ , \qquad \text{(A11)}$$

where $|n\rangle$ (or $|m\rangle$) specifies a three-body state, and is the solution of the three-body equation on the rotated contour while 1 and 3 are defined in (A1). The propagator τ can be related to the on-shell t matrix by

$$\tau_{3n}(P^2/2\mu_{\alpha p})=t_{3n}(p,p,p^2/2\mu_{\alpha p})g_{3n}{}^{-2}(p)\ . \qquad \text{(A12)}$$

In order to obtain the factor $\langle \vec{q}\,|\,Z\tau X\,|\,\vec{q}_{in}\rangle$, we must perform an integration over the intermediate momentum $\vec{q}\,'$ which reduces the importance of the details of the two-body t matrix. On the contrary, the factor $q\tau$ in formula (A11) as well as T_3 in formula (A7) are functions of the relative p-α momentum $\vec{p}$ and, hence, their on-shell value is important.

In the present paper we calculate the factor $\langle \vec{q}\,|\,Z\tau X\,|\,q_{in}\rangle$ by solving the three-body equation with the Yamaguchi-type separable potential which fits the low energy two-body scattering data. In the type I calculation the same potential is used for $g\tau$ in Eq. (A11) and T_3 in Eq. (A6). In the type II and III calculations we modify $g\tau$ and T_3 as discussed in the text.

[1]L. D. Faddeev, Zh. Eksp. Teor. Fiz. 39, 1459 (1960) [Sov. Phys.—JETP 12, 1014 (1961)].

[2]D. Lehman, M. Rai, and A. Ghovanlou, Phys. Rev. C 17, 744 (1978); J. Bang and C. Gignoux, Nucl. Phys. A313, 119 (1979).

[3]A. Ghovanlou and D. Lehman, Phys. Rev. C 9, 1730 (1974).

[4]B. Charnomordic, C. Fayard, and G. H. Lamot, Phys. Rev. C 15, 864 (1977).

[5]Y. Koike, Prog. Theor. Phys. 59, 87 (1978); Y. Koike, in *Few Body Systems and Nuclear Forces,* edited by H. Zingl *et al.* (Springer, Berlin, 1978), Vol. I, p. 320; Y. Koike, Nucl. Phys. A301, 411 (1978).

[6]M. I. Haftel, R. G. Allas, L. A. Beach, R. O. Bondelid, E. L. Petersen, I. Slaus, J. M. Lambert, and P. A. Treado, Phys. Rev. C 16, 42 (1977).

[7]R. H. Bassel and M. I. Haftel, in *Few Body Systems and Nuclear Forces,* edited by H. Zingl *et al.* (Springer, Berlin, 1978), Vol. I, pp. 325, 327.

[8]E. Karaoglan, L. T. Myers, J. M. Lambert, P. A. Treado, M. I. Haftel, I. Slaus, P. G. Roos, A. Nadasen, T. A. Carey, and N. S. Chant, in *Few Body Systems and Nuclear Forces* edited by H. Zingl *et al.* (Springer, Berlin, 1978), Vol. I, p. 239.

[9]S. K. Young and E. F. Redish, Phys. Rev. C 10, 498 (1974).

[10]H. Nakamura, H. Noya, S. E. Dardin, and S. Sen, Nucl. Phys. A305, 1 (1978).

[11]H. Oswald, W. Burgmer, D. Gola, C. Heinrich, H. J. Helton, H. Paetz gen-Schieck, and Y. Koike, Phys. Rev. Lett. 46, 307 (1981).

[12]A. Nadsen, T. A. Carey, P. G. Roos, N. S. Chant, C. W. Wang, and H. L. Chen, Phys. Rev. C 19, 2099 (1979).

[13]E. Hourany, H. Nakamura, F. Takeutchi, and T. Yuasa, Nucl. Phys. A222, 537 (1974).

[14]K. Sagara, T. Motobayashi, N. Takahashi, Y. Hashimoto, M. Hava, Y. Nogami, H. Nakamura, and H. Noya, Nucl. Phys. A299, 77 (1978).

[15]I. Koersner, L. Glantz, A. Johansson, B. Sundguist, H. Nakamura, and H. Noya, Nucl. Phys. A286, 431 (1977); L. Glantz *et al.*, contributed paper to the *Proceedings of the IX International Conference on the Few Body Problem,* edited by M. J. Moravesik and F. S. Levin (University of Oregon, Eugene, 1980), Vol. I.

[16]K. Sagara, T. Motobayashi, N. Takahashi, Y. Hashimoto, M. Hara, Y. Nogami, H. Nakamura, and H. Noya, Nucl. Phys. A237, 493 (1976); K. Saraga, M. Hara, N. Takashashi, T. Motobayashi, F. Takeutchi, F. Soga, and Y. Nogami, J. Phys. Soc. Jpn. 42, 732 (1977).

[17]K. Prescher, W. Bretfeld, W. Burgmer, H. Eicner, H. Helton, H. Klein, H. Kretzer, H. Steehle, and W. W. Wohlprarth, Nucl. Phys. A286, 142 (1977).

[18]T. Rausch, H. Zell, D. Wallenwein, and W. von Witsch, Nucl. Phys. A222, 429 (1974).

[19]T. Tanabe, J. Phys. Soc. Jpn. 25, 21 (1968).

[20]R. E. Warner and R. W. Bercaw, Nucl. Phys. A109, 205 (1978).

[21]D. I. Bonbright, Ph.D. thesis, University of Maryland, 1970 (unpublished).

[22]R. G. Allas, D. I. Bonbright, R. O. Bondelid, E. L. Petersen, A. G. Pieper, and R. B. Theus, Phys. Rev. Lett. 28, 569 (1972).

[23]S. S. Dasgupta, R. J. Slobodrian, R. Roy, C. Rioux, and F. Lahlove, Phys. Rev. C 22, 1815 (1980); Phys. Lett. 91B, 32 (1980).

[24]M. Bruno, F. Cannata, M. D'Agostino, G. Vannini, M. Lombardi, and Y. Koike, Lett. Nuovo Cimento 29, 385 (1980).

[25]H. Nakamura, Nucl. Phys. A208, 207 (1973); A223, 599 (1974).

[26]I. Slaus, R. G. Allas, L. A. Beach, R. O. Bondelid, E. L. Petersen, J. M. Lambert, P. A. Treado, and R. A. Moyle, Nucl. Phys. A286, 67 (1977).
[27]G. R. Satchler, L. W. Owens, A. J. Elwyn, G. L. Morgan, and R. L. Walter, Nucl. Phys. A112, 1 (1968); G. E. Thompson, M. B. Epstein, and T. Sawada, *ibid.* A142, 571 (1970), and references therein.
[28]K. Koike, Prog. Nucl. Phys. A227, 23 (1980).
[29]E. O. Alt, P. Grassberger, and W. Sandhas, Nucl. Phys. B2, 167 (1967).
[30]J. H. Hetherington and L. H. Schick, Phys. Rev. B 935, 137 (1965).
[31]C. Cattapan, G. Pisent, and V. Vanzani, Nucl. Phys. A241, 204 (1975).
[32]R. A. Arndt, L. D. Roper, and R. L. Shotwell, Phys. Rev. C 3, 2000 (1971).
[33]R. A. Arndt, D. D. Long, and L. D. Roper, Nucl. Phys. A209, 429 (1973).
[34]A. Houdayer, N. E. Davison, S. A. Elbakr, A. M. Sourkes, W. T. H. van Oers, and A. D. Bacher, Phys. Rev. C 18, 1985 (1978); D. C. Dodder, G. M. Hale, N. Jarmie, J. H. Jett, P. W. Keaton, R. A. Niseley, and K. Witte, Phys. Rev. C 15, 518 (1977).
[35]M. Brown, M. S. thesis, Georgetown University, 1979 (unpublished).
[36]L. T. Myers, Ph.D. thesis, Georgetown University, 1979 (unpublished).
[37]L. T. Myers, J. M. Lambert, P. A. Treado, I. Slaus, E. W. Devins, and E. Harper (unpublished).
[38]D. F. Measday and R. J. Schneider, Nucl. Instrum. Methods 42, 26 (1966); A. M. Sourkes, M. S. deJong, C. A. Goulding, W. T. H. van Oers, E. A. Ginkel, R. F. Carlson, A. J. Cox, and D. J. Margaziotis, *ibid.* 143, 589 (1977).
[39]J. N. Palmieri and J. Wolfe, Nucl. Instrum. Methods 76, 55 (1969).
[40]Y. Koike, Ph.D. thesis, Kyoto University, 1978 (unpublished).
[41]K. Wick, European Conference on Few Body Problems, Fenara, Italy, 1981 (unpublished).